BJR

https://doi.org/10.1259/bjr.20190712

Received: 14 August 2019 | Revised: 06 November 2019 | Accepted: 29 November 2019

Cite this article as:
Hayashi Y, Satake H, Ishigaki S, Ito R, Kawamura M, Kawai H, et al. Kinetic volume analysis on dynamic contrast-enhanced MRI of triple-negative breast cancer: associations with survival outcomes. *Br J Radiol* 2020; **93**: 20190712.

FULL PAPER

Kinetic volume analysis on dynamic contrast-enhanced MRI of triple-negative breast cancer: associations with survival outcomes

YOKO HAYASHI, MD, HIROKO SATAKE, MD, PhD, SATOKO ISHIGAKI, MD, PhD, RINTARO ITO, MD, PhD, MARIKO KAWAMURA, MD, PhD, HISASHI KAWAI, MD, PhD, SHINGO IWANO, MD, PhD and SHINJI NAGANAWA, MD, PhD

Department of Radiology, Nagoya University Graduate School of Medicine, Nagoya, Japan

Address correspondence to: Dr Yoko Hayashi
E-mail: *hayashi.yoko@med.nagoya-u.ac.jp*

Objective: To evaluate the associations between computer-aided diagnosis (CAD)-generated kinetic volume parameters and survival in triple-negative breast cancer (TNBC) patients.
Methods: 40 patients with TNBC who underwent preoperative MRI between March 2008 and March 2014 were included. We analyzed CAD-generated parameters on dynamic contrast-enhanced MRI, visual MRI assessment, and histopathological data. Cox proportional hazards models were used to determine associations with survival outcomes.
Results: 12 of the 40 (30.0%) patients experienced recurrence and 7 died of breast cancer after a median follow-up of 73.6 months. In multivariate analysis, higher percentage volume (%V) with more than 200% initial enhancement rate correlated with worse disease-specific survival (hazard ratio, 1.12; 95% confidence interval, 1.02–1.22; *p*-value, 0.014) and higher %V with more than 100% initial enhancement rate followed by persistent curve type at 30% threshold correlated with worse disease-specific survival (hazard ratio, 1.33; 95% confidence interval, 1.10–1.61; *p*-value, 0.004) and disease-free survival (hazard ratio, 1.27; 95% confidence interval, 1.12–1.43; *p*-value, 0.000).
Conclusion: CAD-generated kinetic volume parameters may correlate with survival in TNBC patients. Further study would be necessary to validate our results on larger cohorts.
Advances in knowledge: CAD generated kinetic volume parameters on breast MRI can predict recurrence and survival outcome of patients in TNBC. Varying the enhancement threshold improved the predictive performance of CAD generated kinetic volume parameter.

INTRODUCTION

Triple-negative breast cancer (TNBC) is defined by a lack of overexpression of estrogen receptor (ER), progesterone receptor (PR), and human epidermal growth factor receptor-2 (Her2). TNBC is mostly an aggressive subgroup,[1] but this is in fact widely heterogeneous, and the prognosis varies according to clinical, pathological, and genetic factors.[2] Peak recurrence occurs within the first 3 years, whereas late recurrence declines over the following 5 years,[3] and patients who remain disease-free over 8 years are unlikely to die from breast cancer.[4] Many efforts have been assessed to clarify risk stratification in patients with TNBC. Pathological complete response (pCR) rates after neoadjuvant chemotherapy (NAC) have been shown to be higher in patients with TNBC compared with patients with estrogen receptor-positive breast cancers.[5,6] However, a response other than pCR or near-pCR increase the risk of recurrence and death in TNBC patients compared with non-TNBC patients.[5] Larger tumor size, lymph node metastasis, lymphatic invasion, and advance stage has been observed as clinicopathological risk factors for recurrence of TNBC.[7–9] One of the most extensively investigated factors is androgen receptor (AR),[10,11] but this marker is not used in routine practice. Recently, tumor-associated stroma have been recognized to influence tumor malignant behavior including progression, invasion and metastasis.[12] Tumor–stromal ratio (TSR) is a parameter of the amount of tumor-associated stroma, which has proved to be a poor prognostic factor of invasive breast cancer, and the most pronounced prognostic effect of this has been observed in TNBC.[13–15] TSR has been reported to be an independent variables of recurrence and death in TNBC.[16]

Dynamic contrast-enhanced MRI (DCE-MRI) has been believed to have the ability to assess tumor vascularity

and the extracellular extravascular space (EES) induced by the neoplasm through MRI-derived kinetic parameters. Recently, several studies have reported that these kinetic parameters correlate with breast cancer prognostic factors or survival.[17–22] Yamaguchi et al reported the correlations of TSR in invasive breast cancers with DCE-MRI findings. In their study, invasive breast cancers with high-stroma had higher percentage of kinetic component with a delayed persistent curve pattern.[23] On the other hand, in assessing breast DCE-MRI, computer-aided diagnosis (CAD) programs have been developed to overcome the subjectivity inherent in visual assessment.[24,25] These programs automatically generate kinetic curves and provide detailed information about the cancer lesion. Previous studies have shown correlations between CAD-generated kinetic parameters and survival of patients with breast cancers.[26–28] As shown in those studies, in CAD kinetic curve assessment, enhancement rate thresholds are commonly set according to the definitions of the American College of Radiology Breast Imaging Reporting and Data System (BI-RADS) MRI criteria. However, in recent CAD assessment studies with treatment response of breast cancer after NAC, thresholds were changed and optimized, and thus differed from those defined by the BI-RADS definitions.[29–31] If we set the thresholds for initial and delayed phases higher than those defined by the BI-RADS definitions, kinetic components with higher blood flow and with higher stroma could be segmented automatically by CAD.

The purpose of this study was to evaluate associations between CAD-generated kinetic volume parameters and survival in TNBC patients, and to identify more optimal DCE-MRI biomarkers for risk stratification of TNBC.

METHODS AND MATERIALS

Study population

Our institutional review board approved this study, and the requirement for informed consent was waived. From our hospital (Nagoya University Hospital) database, we identified 49 patients with a pathologic diagnosis of TNBC who had undergone surgery with pretreatment DCE-MRI at our institution between March 2008 and March 2014. Seven patients who underwent MRI using different DCE protocols were excluded. Two patients who had incomplete CAD-generated images for analysis were also excluded. As a result, a final total of 40 patients (all female) with TNBC who underwent pretreatment DCE-MRI in a same protocol were included as our study population.

MR imaging

All patients were scanned in a prone position using a 3 T MRI scanner (MAGNETOM Trio; Siemens Medical Solutions, Erlangen, Germany) with a dedicated 4-channel phased-array bilateral breast coil. Before administration of contrast media, axial bilateral images were acquired using a fat-suppressed T_2 weighted fast spin echo sequence. Dynamic axial bilateral breast images of fat-suppressed T_1 weighted three-dimensional fast gradient-echo images (VIEWS) were sequentially acquired before and 75, 185 and 295 s after administration of the contrast medium. Gadopentetate dimeglumine (Magnevist; Bayer Schering, Osaka, Japan) was administered intravenously at a dose of 0.1 mmol/kg body weight and a flow rate of 2 ml s^{-1}, followed by a 20 ml saline flush. Parameters of the VIEWS sequence were as follows: repetition time, 4.2 ms; echo time, 1.6 ms; flip angle, 15°; field of view, 340 × 340 mm; matrix, 512 × 410; thickness, 0.9 mm; one acquisition; and acquisition time, 110 s. SPAIR for fat suppression and a GRAPPA acceleration factor of 2 for parallel imaging were also applied.

MRI analysis

All dynamic axial bilateral breast MRI were transferred to a dedicated CAD system (syngo BreVis; Siemens Medical Solutions) and retrospectively processed. This CAD system automatically calculated kinetic enhancement curve for each voxels, and created a color map semi-quantitatively according to the setting thresholds of initial enhancement (*i.e.*IE) rate and delayed kinetic curve type (Figure 1). IE rate was defined as $(SI_{1st} - SI_{pre}) / SI_{pre} * 100$, where SI_{1st} is the signal intensity of the identified voxel in the first post-contrast series (obtained at 75 s after contrast injection), and SI_{pre} is the signal intensity of the pre-contrast measurement. Delayed kinetic curve types were classified into three types: persistent; plateau; and washout. A persistent curve type indicated an increase in voxel signal intensity greater than the threshold at the third post-contrast series (obtained at 295 s after contrast injection) compared to the first post-contrast series. A washout curve type indicated a decrease in voxel signal intensity greater than the threshold at the third post-contrast series from the first post-contrast series. A plateau curve type indicated an increase or decrease in voxel signal intensity below the threshold. Except determining the values of thresholds, these steps were automatically performed by the CAD system. A sphere volume of interest (VOI) was placed manually to enclose the whole lesion. When necessary, non-cancerous region of enhancement intruding on the VOI, such as extremely strong background parenchymal enhancement or vessels were eliminated using a manually drawn irregular VOI. Setting the VOI, total enhanced volume (TEV (cm^3)), which was defined in this study to be the volume of all voxels exceeding an IE rate of 50%, was calculated and recorded. Simultaneously, each percentage volume (%V; the percentage of a volume meeting the threshold for IE rate and delayed curve type) relative to TEV were calculated. Thresholds for IE rate and curve type were modifiable, and were set at 100 and 10% according to BI-RADS criteria. We also investigated setting the IE threshold at 200% and the delayed curve type threshold at 30%. As the variables of kinetic volume analysis in initial phase, we selected %V of more than 100% (>100%) and 200% (>200%) IE rate. As the variables of kinetic volume analysis through the initial and delayed phase, %V meeting thresholds for combinations of >100% or >200% IE rate and subsequent curve type (persistent, plateau, and washout) were recorded. Ultimately, investigated CAD kinetic volume parameters in this study were as follows.

- TEV(cm^3)
- %V >100% IE rate
- %V >200% IE rate
- %V >100% IE rate - < -10% washout (decrease in signal intensity of more than 10%)

Figure 1. Pretreatment MR images overlaid with CAD color maps based on varying thresholds of IE and delayed kinetic curve types. (a, b, (c). A 48-year-old female with triple negative breast cancer who was found to have no recurrence after a follow-up 2573 days. (d, e, f), A 48-year-old female with triple negative breast cancer who was found to have distant recurrence after a follow-up 41 days and died after 111 days. (a, d) Axial contrast-enhanced MR image overlaid with CAD color map based on IE threshold at 200%. Areas in red indicate fast enhancement with >200% IE rate. (b, e) Axial contrast-enhanced MR image overlaid with CAD color map based on IE threshold at 100% and curve type (persistent, plateau, and washout) at 30% threshold. Light blue areas indicate with >100% IE rate followed by persistent curve type with >30% signal increase. Setting the VOI, TEV (the volume of all voxels exceeding an IE rate of 50%) (cm^3), percentage volume (%V; the percentage of a volume meeting the threshold for IE and delayed curve type) were calculated automatically. (c, f) Results of %V. In the diagrams, the ordinate shows IE rate and its threshold. The abscissa shows delayed kinetic curve types and the thresholds. Percentage indicates %V which is proportion meeting the thresholds to TEV %V with >100% IE rate followed by persistent curve type at 30% threshold was 0.6% in (c), and 22.7% in (f). CAD, computer-aided diagnosis; IE, initial enhancement; TEV, total enhanced volume; VOI, volume ofinterest.

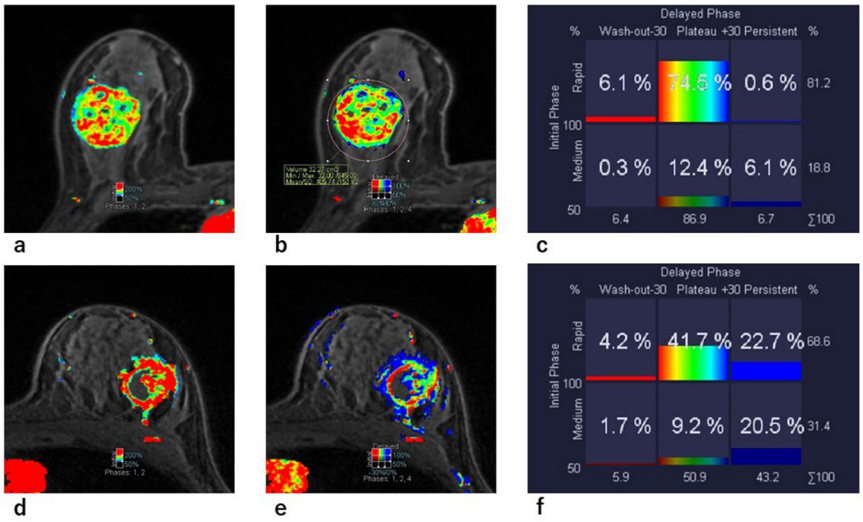

- %V >100% IE rate - ±10% plateau (signal intensity that remained within ± 10%)
- %V >100% IE rate - > 10% persistent (increase in signal intensity of more than 10%)
- %V >100% IE rate - < -30% washout (decrease in signal intensity of more than 30%)
- %V >100% IE rate - ±30% plateau (signal intensity that remained within ± 30%)
- %V >100% IE rate - >30% persistent (increase in signal intensity of more than 30%)
- %V >200% IE rate - < -10% washout
- %V >200% IE rate - ±10% plateau
- %V >200% IE rate - >10% persistent
- %V >200% IE rate - < -30% washout
- %V >200% IE rate - ±30% plateau
- %V >200% IE rate - > 30% persistent

Visual MRI assessment was performed by reviewing mass shape (irregular or round/oval), mass margin (not circumscribed or circumscribed), and internal enhancement (heterogeneous or rim enhancement). In addition, the presence of intratumoral signal hyperintensity and the presence of peritumoral edema on T_2 weighted images were also determined. One dedicated breast radiologist (HS, with 25 years of experience of breast imaging) performed, first, CAD analysis, and visual assessments separately after more than a month. The diagnosis of TNBC was known, but the reader was blinded regarding survival, presence of metastasis, and other clinical/histopathological data.

Data collection

We collected patient's age, race, clinical tumor size, surgery type, receipt of radiation and/ or chemotherapy, time and site of recurrence, time of breast cancer death, and last follow-up from the patient's medical record. We defined clinical tumor size as the largest diameter measured by MRI. The pathologic tumor size, histologic type, nuclear grade, presence of lymphovascular invasion, surgical margin status, axillary lymph node status, and the expression status of ER, PR, and HER2 were obtained from pathology reports for surgical or core biopsy samples obtained prior to initiating NAC. For the expression statuses of ER, PR, the presence at least 1% positive tumor nuclei in a sample was used to define ER and PR positivity.[32] The intensity of immunohistochemical staining for HER2 was initially scored as 0, 1+, 2+, or 3+, with tumors scoring 0 or 1+ classified as HER2-negative. Gene amplification using fluorescence *in situ* hybridization was performed in tumors with a score of 2+ to determine HER2 status.[33] TNBC was defined as a tumor showing negative results for ER, PR, and HER2.

Surveillance and follow-up

For the surveillance of locoregional or contralateral breast recurrence, we examined patients annually with mammography and

ultrasonography. Chest radiography, chest and abdomen CT, or whole-body fluorine 18-fludeoxyglucose positron emissiontomography was performed for surveillance of distant metastasis. Recurrence was defined as locoregional (limited to the ipsilateral breast or chest wall and/or to the axillary, infraclavicular, or supraclavicular, or internal mammary lymph nodes), contralateral breast, or distant (metastasis to other parts of the body), according to the first pathologically detected recurrence site in each patient.

Statistical analysis

The primary outcomes were disease-free survival (DFS) and disease-specific survival (DSS). DFS was defined as the time from the date of surgery to the date of first recurrence of breast cancer. In the absence of events, DFS was calculated as the interval between the date of surgery and the last clinical follow-up. DSS was defined as the time from surgery to death from breast cancer, or to the date of last follow-up.

Patient characteristics were compared between patients with and patients without recurrence, and between patients with and patients without death from breast cancer, by using a $\chi 2$ test or Fisher exact test. For continuous variables, the Shapiro–Wilk test and Levene F test were performed for normality and equal variance. If the data were normally distributed and had equal variance, the Student's *t*-test was used. Otherwise, the Mann–Whitney *U* test was performed. Cox proportional hazards modeling was used to analyze DFS and DSS with CAD-generated kinetic volume parameters (TEV, and %V), visual MRI assessment, and clinicopathological data (clinical tumor size, cancer type (invasive ductal carcinoma, IDC or others), lymphovascular invasion, nuclear grade (3 *vs* 1 or 2), and LN metastasis). When univariate analysis identified a factor showing a value of $p < .05$, that factor was selected as a candidate for addition to the multivariate Cox proportional hazards model. Because of expected multicollinearity, we selected variables with showing the lower *p*-value among significant kinetic volume parameters at univariate analysis, and inserted into the multivariate model separately a variable of % $V >$ IE rate and a variable of % $V >$ IE with delayed curve type.

On the basis of receiver operating characteristic (ROC) curve analysis, optimal cut-off values for kinetic volume parameters were determined by checking the point closest to the (0,1). Using the cut-off values, we dichotomized into two groups and generated Kaplan–Meier survival curves. Differences between survival curves were examined using the log-rank test.

Statistical analyses were conducted using SPSS Statistics v. 23.0 software (IBM, Chicago, IL).

RESULTS

Patients characteristics and outcomes

Clinical and pathological characteristics among 40 patients are shown in Table 1. The mean age of the patients was 56.1 years (range: 32–77 years) and all were East Asians. Genetic testing for BRCA mutation was not performed in all 40 patients. The mean of clinical tumor size measured at MR imaging was 2.615 cm (range: 0.9–10.0 cm). Of 35 (87.5%) patients who underwent adjuvant chemotherapy, six patients received NAC before surgery and one patient achieved pathologic complete response. Among all 40 patients, partial mastectomy was performed in 20 patients (50.0%) and total mastectomy was performed in 20 patients (50.0%). In all 20 patients who underwent partial mastectomy, surgical margin status was negative of cancer cells. 18 patients (45.0%) underwent adjuvant intra- or postoperative radiotherapy.

Median follow-up for all patients was 73.6 months (range, 3.7–105.9 months). Disease recurred in 12 patients (30.0%), at a median of 32.5 months follow-up (range, 1.4–61.5 months). Two patients experienced locoregional recurrence, six had distant recurrence, two had both locoregional and distant recurrence, and two had contralateral breast cancer. Of the 12 patients who experienced recurrence, 7 patients died of breast cancer at a median of 50.3 months of follow-up (range, 3.7–64.3 months).

Compared with patients without breast cancer death, patients with breast cancer death had significantly more cases of axillary lymph node metastasis (*p*-value, 0.011) and lymphovascular invasion (*p*-value, 0.034). Compared with patients without recurrence, patients with recurrence had significantly more cases of axillary lymph node metastasis (*p*-value, 0.047). No significant differences were found regarding age (*p*-value, 0.144; 0.220), clinical tumor size (*p*-value, 0.149; 0.117), nuclear grade (*p*- value, 0.592; 0.609), histologic type (*p*- value, 0.361; 0.523), surgery type (*p*- value, 0.500; 0.490), chemotherapy (*p*- value, 0.361;, 0.523), and radiation therapy (*p*- value, 0.383; 0.944) status between the death and no death group, and between the recurrence and no recurrence group.

DSS analysis

Tables 2–4 shows the results of associating variables with DSS and DFS in univariate analysis. Higher %V with the >200% IE rate was associated with worse DSS [hazard ratio (HR), 1.12; 95% confidence interval (CI), 1.03–1.21; *p*-value, 0.011]. In combination with delayed curve types, higher %V with >100% or >200% IE rate followed by a persistent curve type was significantly associated with worsened DSS, irrespective of whether the threshold was 10% or 30%. On the other hand, higher %V with >100% or >200% IE rate followed by a washout curve type was not significantly associated with worsened DSS, irrespective of whether the threshold was 10% or 30%. TEV (HR, 1.04; 95% CI, 0.98–1.09; *p*-value, 0.19) of lesions was not significantly associated with DSS (Table 4).

Visual MRI assessment showed no variables associated with DSS (Table 3). Of the histopathological data, presence of lymphovascular invasion (HR, 6.45; 95% CI, 1.43–29.17; *p*-value, 0.015) and presence of LN metastasis (HR, 10.53; 95% CI, 2.00–55.44; *p*-value, 0.005) were both associated with worsened DSS (Table 2).

As input variables for multivariate analysis, we selected %V at the >200% IE rate. Furthermore, since the *p*-value was the smallest, we selected %V at the >100% IE rate followed by persistent curve type at the 30% threshold (>30% persistent) (HR, 1.30; 95% CI, 1.12–1.52; *p*-value, 0.001), and these were analyzed separately

Table 1. Patient Characteristics of 40 Patients according to Breast Cancer Death and Recurrence

Variable	ALL Patients (*n* = 40)	Breast cancer death (*n* = 7)	No breast cancer death (*n* = 33)	*p*-value	Recurrence (*n* = 12)	No recurrence (*n* = 28)	*p* -value
Age at diagnosis	56.1 ± 10.9*	49.0 ± 10.5*	57.61 ± 10.7*	0.144	52.17 ± 11.13*	57.79 ± 10.36*	0.220
Clinical tumor size	2.62 ± 1.7 cm*	3.00 ± 1.23 cm*	2.53 ± 1.82 cm*	0.149	3.08 ± 1.64 cm*	2.41 ± 1.75 cm*	0.117
Axillar LN metastasis				0.011			0.047
No	29 (72.5)	2 (28.6)	27 (81.8)		6 (50.0)	23 (82.1)	
Yes	11 (27.5)	5 (71.4)	6 (18.2)		6 (50.0)	5 (17.9)	
Nuclear grade				0.592			0.609
1 or 2	13 (32.5)	2 (28.6)	11 (50.0)		4 (33.3)	9 (32.1)	
3	27 (67.5)	5 (71.4)	22 (50.0)		8 (66.7)	19 (67.9)	
Lymphovascular invasion				0.034			0.072
Absent	31 (77.5)	3 (42.9)	28 (84.8)		7 (58.3)	24 (85.7)	
Present	9 (22.5)	4 (57.1)	5 (15.2)		5 (41.7)	4 (14.3)	
Histologic type				0.361			0.523
IDC	35 (87.5)	7 (100)	28 (84.8)		11 (91.7)	24 (85.7)	
Others	5 (12.5)	0 (0)	5 (15.2)		1 (8.3)	4 (14.3)	
Surgery type				0.500			0.490
Partial mastectomy	20 (50.0)	4 (57.1)	16 (48.5)		6 (50.0)	14 (50.0)	
Total mastectomy	20 (50.0)	3 (42.9)	17 (51.5)		6 (50.0)	14 (50.0)	
Adjuvant chemotherapy				0.361			0.523
No	5 (12.5)	0 (0)	5 (15.2)		1 (8.3)	4 (14.3)	
Yes	35 (87.5)	7 (100)	28 (84.8)		11 (91.7)	24 (85.7)	
Adjuvant radiotherapy				0.383			0.944
No	22 (55.0)	3 (42.9)	19 (57.6)		7 (58.3)	14 (50.0)	
Yes	18 (45.0)	4 (57.1)	14 (42.4)		5 (41.7)	14 (50.0)	

IDC, invasive ductal cancer; LN, lymph node.
Unless otherwise noted, values are the numbers of patients, with percentages in parentheses. * Data are mean ± standard deviation

Table 2. Clinical and pathological factors associated with DSS and DFS at univariate analysis

	DSS status		DFS status	
Variable	**HR (95% CI)**	*p*- value	**HR (95% CI)**	*p*- value
Clinical tumor size	1.09 (0.78–1.52)	0.606	1.15 (0.91–1.45)	0.246
Axillar LN metastasis				
No	1		1	
Yes	10.53 (2.00–55.44)	0.005	4.04 (1.29–12.64)	0.016
Nuclear grade				
1 or 2	1		1	
3	1.21(0.23–6.21)	0.824	0.92 (0.28–3.05)	0.887
Lymphovascular invasion				
Absent	1		1	
Present	6.45 (1.43–29.18)	0.015	3.53 (1.11–11.21)	0.032
Histologic type				
IDC	1		1	
others	24.02(0.00–1532932.27)	0.573	1.66 (0.21–12.86)	0.630

CI, confidence interval; DFS, disease-free survival; DSS, disease-specific survival; HR, hazard ratio; IDC, invasive ductal cancer;LN, lymph node.

(Tables 2, 3, 5 and 6). In multivariate analysis, higher %V at the >200% IE rate was independently associated with worsened DSS (HR, 1.12; 95% CI, 1.02–1.22; *p*-value, 0.014). In the other multivariate analysis, higher %V at the >100% IE rate followed by >30% persistent was another independent variable associated with worsened DSS (HR, 1.33; 95% CI, 1.10–1.61; *p*-value, 0.004).

DFS analysis

Of the CAD kinetic volume parameters in univariate analyses, higher %V at the >100% or >200% IE rate followed by persistent curve type was significantly associated with worsened DFS, irrespective of whether the threshold for persistent curve type was 10% or 30%. TEV of lesions (HR, 1.04; 95% CI, 1.00–1.09; *p*-value, 0.052) and %V of delayed washout pattern were not significantly associated with DFS (Table 4). Of the histopathological data, presence of lymphovascular invasion (HR, 3.53; 95% CI, 1.11–11.21; *p*-value, 0.032) and presence of LN metastasis (HR, 4.04; 95% CI, 1.29–12.64; *p*-value, 0.016) were both associated with worsened DFS (Table 2).

As input variables for multivariate analysis, since the *p*-value was the smallest, we selected the %V at the >100% IE rate followed by >30% persistent (HR, 1.23; 95% CI, 1.11–1.36; *p*-value, 0.000). Multivariate analysis revealed higher %V at the >100% IE rate followed by >30% persistent as independently associated with worsened DFS (HR, 1.27; 95% CI, 1.12–1.43; *p*-value, 0.000) (Table 7).

ROC curve analysis and Kaplan–Meier survival analysis

ROC curve analysis of DSS revealed the optimal cut-off values for %V at the >200% IE rate and >100% IE rate followed by >30% persistent were 17.5 and 7.5%, respectively. Using these cut-off values, patients were divided into two groups. Results of Kaplan–Meier survival (Figure 2) analysis indicated that TNBC patients with a higher %V at the >200% IE rate (≥17.5%) or higher %V at the >100% IE rate followed by >30% persistent (≥7.5%) on pre-operative MRI showed significantly worse DSS (p = 0.014 and 0.004).

In association with DFS, the optimal cut-off value for %V at the >100% IE rate followed by >30% persistent was 7.5%. Using this cut-off, patients were divided into two groups and Kaplan–Meier survival analysis (Figure 3) indicated that patients with tumors with a $\%V \geq 7.5\%$ at the >100% IE rate followed by >30% persistent displayed significantly worse DFS (p = 0.000).

DISCUSSION

Our data showed that higher %V at the >200% IE rate correlated independently with worsened DSS in patients with TNBC. A recent study showed that mean peak enhancement rate in the tumor was significantly associated with worsened DSS in patients with TNBC.[17] Some other studies including patients with both non-TNBC and TNBC reported peak enhancement rate to be associated with poor prognosis.[26,34] Both peak enhancement and IE rate are considered to reflect the concentration of contrast agent on early DCE-MRI in both the intravascular and EES, which are dependent on tumor angiogenesis. Histopathologically, high correlations between angiogenic markers, such as microvessel density or vascular endothelial growth factor, and overall outcomes for patients with breast cancer have been explored in previous studies.[35–37] These results could explain the relationship between IE or peak enhancement rate and poor prognosis of breast cancers. We believe our study could semi-quantify tumor angiogenesis through DCE-MRI using CAD systems, and provided evidence that a greater component with a high IE rate was associated with worsened DSS in patients with TNBC (Figure 1(a),(d)). Volume measurements based on DCE-MRI with setting thresholds for kinetic curve parameters (kinetic

Table 3. Visual MRI assessment associated with DSS and DFS at univariate analysis

	DSS status				DFS status			
Variable	**Breast cancer death* (*n* = 7)**	**No Breast cancer death* (*n* = 33)**	**HR (95% CI)**	*p*- value	**Recurrence* (*n* = 12)**	**No recurrence* (*n* = 28)**	**HR (95% CI)**	*p*- value
Mass shape								
Round or oval	0 (0.0)	13 (39.4)	1		1 (8.3)	12 (42.9)	1	
Irregular	7 (100.0)	20 (60.6)	40.01 (0.06–27250.12)	0.728	11 (91.7)	16 (57.1)	2.34 (0.51–10.71)	0.274
Mass margin								
Circumscribed	0 (0)	9 (27.2)	1		0 (0.0)	9 (32.1)	1	
Not circumscribed	7 (100.0)	24 (72.8)	32.68 (0.03–42314.51)	0.340	12 (100.0)	19 (67.9)	33.25 (0.15–7489.42)	0.205
Internal enhancement								
Heterogeneous	4 (57.1)	9 (27.2)	1		5 (41.7)	8 (28.6)	1	
Rim enhancement	3 (42.9)	24 (72.8)	3.06 (0.68–13.73)	0.145	7 (58.3)	20 (71.4)	1.60 (0.51–5.05)	0.423
Intratumoral signal hyperintensity on T_2WI								
Absent	3 (42.9)	24 (72.8)	1		6 (50.0)	21 (75.0)	1	
Present	4 (57.1)	9 (27.2)	2.70 (0.61–12.5)	0.191	6 (50.0	7 (25.0)	2.38 (0.76–7.14)	0.138
Peritumoral edema								
Absent	2 (28.6)	16 (48.5)	1		3 (25.0)	15 (53.6)	1	
Present	5 (71.4)	17 (51.5)	1.95 (0.38–10.10)	0.425	9 (75.0)	13 (46.4)	2.70 (0.74–10.00)	0.132

CI, confidence interval; DFS, disease-free survival; DSS, disease-specific survival; HR, hazard ratio;T_2WI, T_2 weighted imaging.
*Data are the numbers of patients, with percentages in parentheses.

Table 4. CAD kinetic volume parameters associated with DSS and DFS at univariate analysis

	DSS status				DFS status			
Variable	**Breast cancer death* (*n* = 7)**	**No breast cancer death* (*n* = 33)**	**HR (95% CI)**	*p*-value	**Recurrence* (*n* = 12)**	**No recurrence* (*n* = 28)**	**HR (95% CI)**	*p*- value
TEV	16.24 ± 7.91 cm^3	10.10 ± 10.77 cm^3	1.04 (0.98–1.09)	0.189	15.58 ± 11.61 cm^3	9.29 ± 9.51 cm^3	1.04 (1.00–1.09)	0.052
% volume								
>100% IE rate	62.51±9.92%	49.28±18.59%	1.06 (0.99–1.13)	0.114	55.55±14.46%	49.91±19.20%	1.02 (0.98–1.06)	0.299
>200% IE rate	21.57±10.29%	9.66±9.48%	1.12 (1.03–1.21)	0.011	15.56±11.18%	10.11±9.96%	1.05(1.00–1.11)	0.068
>100% IE rate - <-10% washout	14.51±9.99%	15.52±13.70%	0.99 (0.94–1.05)	0.780	11.33±10.07%	17.07±13.90%	0.97 (0.92–1.03)	0.973
>100% IE rate - ± 10% plateau	21.36±3.72%	18.57±7.70%	1.04 (0.94–1.05)	0.992	19.48±6.85%	18.87±7.40%	1.01 (0.94–1.09)	0.756
>100% IE rate - > 10% persistent	26.64±5.71%	15.19±9.48%	1.11 (1.03–1.12)	0.009	24.73±7.07%	13.97±9.21%	1.09 (1.03–1.15)	0.002
>100% IE rate - <-30% washout	2.13±4.16%	1.97±3.32%	1.02 (0.82–1.25)	0.887	1.54±3.38%	2.20±3.51%	0.96 (0.79–1.17)	0.701
>100% IE rate - ± 30% plateau	48.5±6.74%	42.78±15.98%	1.02 (0.96–1.08)	0.494	44.15±10.82%	43.62±16.39%	1.00 (0.97–1.04)	0.840
>100% IE rate - > 30% persistent	11.87±3.19%	4.56±4.04%	1.30 (1.12–1.52)	0.001	9.88±4.36%	4.11±3.83%	1.23 (1.11–1.36)	0.000
>200% IE rate - <-10% washout	8.69±7.07%	5.02±6.68%	1.06 (0.97–1.15)	0.202	5.37±6.51%	5.63±7.05%	1.01 (0.93–1.09)	0.793
>200% IE rate - ± 10% plateau	9.19±3.70%	3.41±3.91%	1.32 (1.08–1.32)	0.008	7.01±4.72%	3.31±3.84%	1.19 (1.04–1.35)	0.009
>200% IE rate - > 10% persistent	3.7±2.69%	1.23±2.16%	1.27 (1.04–1.55)	0.019	2.82±2.44%	1.17±2.27%	1.20 (1.02–1.42)	0.027
>200% IE rate - <-30% washout	0.9±1.88%	0.67±1.74%	1.12 (0.77–1.64)	0.557	0.55±1.50%	0.78±1.86%	0.97 (0.66–1.42)	0.880
>200% IE rate - ± 30% plateau	19.76±8.81%	8.86±8.90%	1.11 (1.02–1.21)	0.014	14.33±9.96%	9.24±9.33%	1.05 (0.99–1.12)	0.076
>200% IE rate - > 30% persistent	0.91±1.23%	0.14±0.30%	3.44 (1.54–7.70)	0.003	0.68±1.02%	0.10±0.23%	3.68 (1.70–7.98)	0.001

CAD, computer-aided diagnosis; CI, confidence interval; DFS, disease-free survival; DSS, disease-specific survival; HR, hazard ratio; IE, initial enhancement; TEV, total enhancement volume.
*Data are mean ± standard deviation.

Table 5. Multivariate analysis including % volume of >200% IE rate, pathological data, and disease-specific survival

Variable	HR (95% CI)	*p*-value
CAD kinetic volume parameters, % volume		
>200% IE rate	1.12 (1.02–1.22)	0.014
Pathological data		
Lymphovascular invasion (+)	2.69 (0.31–23.14)	0.367
Axillar LN metastasis (+)	5.09 (0.47–55.01)	0.180

CI, confidence interval; HR, hazard ratio; IE, initial enhancement;LN, lymph node.

volume measurement) have also been used as predictors of tumor response to NAC of breast cancers.[30,31] For kinetic volume measurement, optimization of the threshold is crucial and varies according to the aims of the evaluation. For the evaluation of tumor response to NAC for breast cancers, a >70% IE rate has frequently been used.[30] According to the kinetic assessment on BI-RADS MRI for predicting of malignancy, the threshold IE rate is defined as 100% between fast and medium enhancement. We speculated that higher blood flow would affect survival for patients with TNBC, and therefore added a fixed threshold of 200% IE rate in addition to the default of 100%. Mean peak enhancement may be influenced by the degree of intratumoral heterogeneity due to various hypovascular components such as necrosis. Maximum peak enhancement value, which has also been used in some studies,[26,34] may reflect the highest perfusion area in the tumor, but cannot evaluate the entire tumor. In comparison, kinetic volume measurements using CAD systems can automatically extract the functional volume of the tumor and evaluate characteristics of the entire tumor three-dimensionally, but further study is needed to clarify the optimal threshold.

In our study, higher %V at the >100% IE rate followed by >30% persistent was another predictor of worsened DSS and was also associated with DFS in patients with TNBC (Figure 1(b), (c), (e),(f)). While no association between delayed persistent curve type and survival on TNBC has been reported, one study found that a higher v_e value was significantly associated with worsened DSS.[17] The v_e value is a pharmacokinetic parameter showing the fractional volume of EES per unit of tissue and has been associated with tumor cellularity and poor prognostic factors in breast cancers.[17,18,38] Histopathologically, v_e values and %V of delayed persistent curve type are reportedly significantly higher in breast cancers with higher stromal percentage.[23,38] Multiple investigators have reported that patients with higher stromal percentage experienced a shorter relapse-free period and shorter overall survival, and these associations were particularly pronounced in patients with TNBC.[13–15] Usually, threshold for the delayed kinetic curve pattern is a 10% increase or decrease in signal intensity, as shown in BIRADS-MRI. Considering the dependence of the EES on TNBC prognosis, we added a 30% increase or decrease in signal intensity as a threshold for the delayed curve pattern. A kinetic curve with the >100% IE rate followed by >30% persistent may reflect initial fast concentration and subsequent high-volume trapping of contrast agent, which may depend on tumor angiogenesis and a high stromal percentage. Furthermore, a recent report found that the delayed persistent curve type correlated with lower levels of tumor-infiltrating lymphocytes (TILs) in patient with TNBC.[39] Multiple investigators have reported that high levels of TILs are significantly associated with better survival outcomes in TNBC.[40,41] Histologically, TIL levels have not been explored in our study, but our result may have association with the levels of TILs.

Table 6. Multivariate analysis including % volume of >100% IE rate followed by > 30% persistent, pathological data, and disease-specific survival

Variable	HR (95% CI)	*p*-value
CAD kinetic volume parameters, % volume		
>100% IE rate - >30% persistent	1.33 (1.10–1.61)	0.004
Pathological data		
Lymphovascular invasion (+)	1.45 (0.12–17.88)	0.770
Axillar LN metastasis (+)	6.00 (0.41–88.86)	0.192

CAD, computer-aided diagnosis; CI, confidence interval; HR, hazard ratio; IE, initial enhancement; LN, lymph node.

Table 7. Multivariate analysis of factors associated with disease-free survival

Variable	HR (95% CI)	*p*-value
CAD kinetic volume parameters, % volume		
>100% IE rate - >30% persistent	1.27 (1.12–1.43)	0.000
Pathological data		
Lymphovascular invasion (+)	1.92 (0.24–15.26)	0.537
Axillar LN metastasis (+)	2.97 (0.37–23.76)	0.304

CAD, computer-aided diagnosis; CI, confidence interval; HR, hazard ratio; IE, initial enhancement; LN, lymph node.

In this study, higher %V at the >100% IE rate followed by >30% persistent was associated with worse results for both DSS and DFS, whereas %V at the >200% IE rate was associated solely with worsened DSS. This is a very interesting result, suggesting that %V at the >200% IE rate offers a predictor of early recurrence with extremely aggressive TNBC. With further validation, more detailed risk stratification in patients with TNBC could be possible using DCE-MRI.

Peritumoral edema on T_2 weighted images is known to be associated with prognostic factors of breast cancer,[42–44] and one report found it correlated significantly with recurrence

Figure 2. Kaplan–Meier survival curves for DSS according to higher % volume (%V) with >200% IE rate and higher %V with >100% IE rate followed by >30% persistent. (a) Curve shows that tumors with %$V \geq 17.5\%$ at the >200% IE rate are associated with worsened DSS ($p = 0.014$). DSS, disease-specificsurvival; IE, initial enhancement. (b) Curve shows that tumors with %$V \geq 7.5\%$ at the >100% IE rate followed by >30% persistent are associated with worsened DSS ($p = 0.004$).

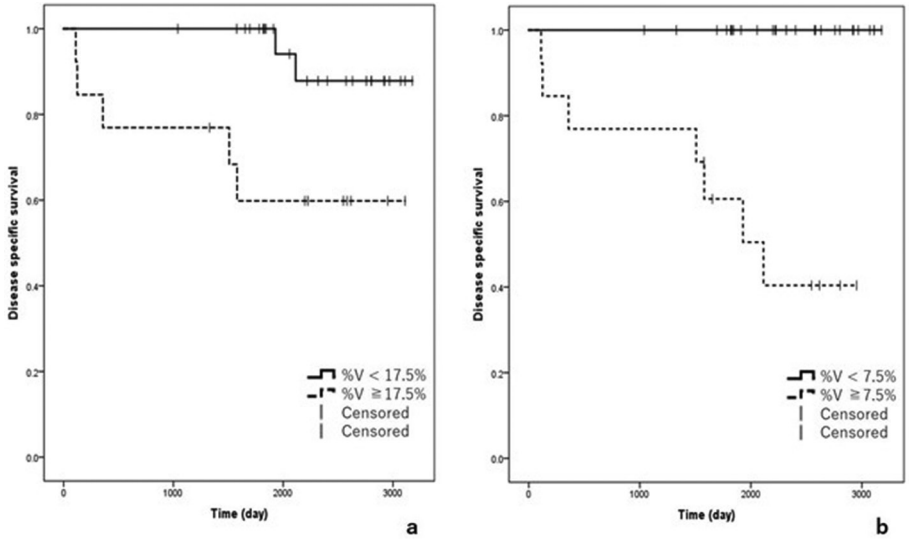

of TNBC. In this study, visual MRI assessments showed no correlations with prognosis. One report found peritumoral edema on T_2 weighted images correlated significantly with recurrence of TNBC,[45] conflicting with the present results. In our study, visual assessment was evaluated by one radiologist subjectively. More observers should have been set and inter- and intraobserver variability should have been evaluated. Therefore our visual result might be caused by subjectivity of the observer. Especially T_2 weighted image interpretation has been reported more subjective.[45] More observers should have been set and inter- and intraobserver variability should have been evaluated. However, completely removing subjectivity from the assessment appears difficult, so we believe using quantitative measurement is a better method for the future. Furthermore, we assessed the CAD-created TEV (cm^3), and found no association with survival. Conversely, maximal diameter (cm) on MRI was reportedly associated with recurrence or DFS of TNBC[17] although it was not significant in our analysis. In such a TNBC with abundant necrosis, inconsistencies may exist between TEV and maximal diameter. Further study is needed to determine predictive parameter of tumor size.

Figure 3. Kaplan–Meier survival curves for DFS according to higher % volume (%V) at the >100% IE rate followed by >30% persistent. Curve shows that tumors with %$V \geq 7.5\%$ at the >100% IE rate followed by >30% persistent are significantly associated with worsened DFS ($p = 0.000$). DFS, disease-freesurvival; IE, initial enhancement.

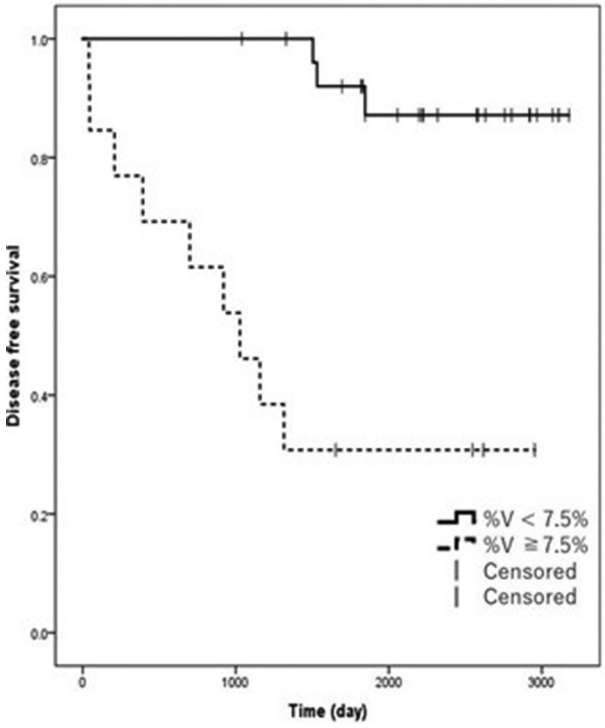

Our study had several limitations. First, this study was retrospective and conducted at a single institution, and the sample size was small. Therefore, the statistical power of the analyses may be insufficient in the study. Especially, since our cohort consisted largely of patients with IDC and the number of other types was extremely small, the results might be affected by a certain degree of this bias. Larger studies are warranted to validate our findings both with a greater number of cases including various types of TNBC. Second, reproducibility issues may have been present in association with semi-quantitative kinetic parameters across different DCE-MRI protocols or different MRI systems.[46] Third, VOI placement was manually by a single radiologist introducing potential operator bias. Operator-dependent differences may increase especially in when surrounding an irregularly shaped tumor or when using an irregular shape VOI modified manually. Further, visual

assessment was also performed by single radiologists. Finally, as already described, the thresholds for IE rate and delayed curve types such as 200 and 30% were not evidence-based. We used the BI-RADS criteria (100 and 10%), then casually added use of the higher threshold. There has been a study which reported IE rate of the high-TIL group in TNBC was lower than that of the low-TIL group in TNBC (195.0±59.093 *vs* 243.54%±138.67%).[14] Referring to only this value, the 200% threshold setting of IE rate in this study may have been roughly appropriate. However, it seems that the threshold needs to be optimized for each study under the same DCE-MRI protocols and systems. For the threshold of curve type in the delayed phase, we have found one study which evaluated association fludeoxyglucose-positron emissiontomography and DCE-MRI findings in TNBC by categorizing kinetic curve patterns in delayed phase with threshold of 30% signal increase or decrease.[47] However, in this study, there were no significant results in persistent kinetic curve with more than 30% signal increase, and their study did not reveal the reason for setting the 30% threshold. Anyways, if we performed analyses under varying threshold statistically, a more optimal threshold could likely be found.

Despite these limitations, this appears to represent the first study to explore CAD-generated kinetic volume measurement of the tumor at varying thresholds, and revealed significant associations with prognostic survival in patients with TNBC.

In conclusion, higher %V at >200% IE rate was independently correlated with worsened DSS, and higher %V at >100% IE rate followed by >30% persistent correlated independently with both worsened DSS and worsened DFS in patients with TNBC. These kinetic volume assessments using CAD have potential utility to predict survival outcomes and to help risk stratification of patients with TNBC, thus enabling personalized clinical decisions for the heterogeneous subgroups of this disease. Further study would be necessary to validate our promising results on larger cohort of patients.

REFERENCES

1. Moran MS. Should triple-negative breast cancer (TNBC) subtype affect local-regional therapy decision making? *Am Soc Clin Oncol Educ Book* 2014; **34**: e32–6. doi: https://doi.org/10.14694/EdBook_AM.2014.34.e32
2. Irshad S, Ellis P, Tutt A. Molecular heterogeneity of triple-negative breast cancer and its clinical implications. *Curr Opin Oncol* 2011; **23**: 566–77. doi: https://doi.org/10.1097/CCO.0b013e32834bf8ae
3. Pistelli M, Pagliacci A, Battelli N, Santinelli A, Biscotti T, Ballatore Z, et al. Prognostic factors in early-stage triple-negative breast cancer: lessons and limits from clinical practice. *Anticancer Res* 2013; **33**: 2737–42.
4. Dent R, Trudeau M, Pritchard KI, Hanna WM, Kahn HK, Sawka CA, et al. Triple-Negative breast cancer: clinical features and patterns of recurrence. *Clin Cancer Res* 2007; **13**(15 Pt 1): 4429–34. doi: https://doi.org/10.1158/1078-0432.CCR-06-3045
5. Liedtke C, Mazouni C, Hess KR, André F, Tordai A, Mejia JA, et al. Response to neoadjuvant therapy and long-term survival in patients with triple-negative breast cancer. *JCO* 2008; **26**: 1275–81. doi: https://doi.org/10.1200/JCO.2007.14.4147
6. von Minckwitz G, Untch M, Blohmer J-U, Costa SD, Eidtmann H, Fasching PA, et al. Definition and impact of pathologic complete response on prognosis after neoadjuvant chemotherapy in various intrinsic breast cancer subtypes. *JCO* 2012; **30**: 1796–804. doi: https://doi.org/10.1200/JCO.2011.38.8595
7. Hernandez-Aya LF, Chavez-MacGregor M, Lei X, Meric-Bernstam F, Buchholz TA, Hsu L, et al. Nodal status and clinical outcomes in a large cohort of patients with triple-negative breast cancer. *JCO* 2011; **29**: 2628–34. doi: https://doi.org/10.1200/JCO.2010.32.1877
8. Pogoda K, Niwińska A, Murawska M, Pieńkowski T. Analysis of pattern, time and risk factors influencing recurrence in triple-negative breast cancer patients. *Med Oncol* 2013; **30**: 388. doi: https://doi.org/10.1007/s12032-012-0388-4
9. Steward L, Conant L, Gao F, Margenthaler JA. Predictive factors and patterns of recurrence in patients with triple negative breast cancer. *Ann Surg Oncol* 2014; **21**: 2165–71. doi: https://doi.org/10.1245/s10434-014-3546-4
10. Loibl S, Müller BM, von Minckwitz G, Schwabe M, Roller M, Darb-Esfahani S, et al. Androgen receptor expression in primary breast cancer and its predictive and prognostic value in patients treated with neoadjuvant chemotherapy. *Breast Cancer Res Treat* 2011; **130**: 477–87. doi: https://doi.org/10.1007/s10549-011-1715-8
11. Pistelli M, Caramanti M, Biscotti T, Santinelli A, Pagliacci A, De Lisa M, et al. Androgen receptor expression in early triple-negative breast cancer: clinical significance and prognostic associations. *Cancers* 2014; **6**: 1351–62. doi: https://doi.org/10.3390/cancers6031351
12. Korkaya H, Liu S, Wicha MS. Breast cancer stem cells, cytokine networks, and the tumor microenvironment. *J Clin Invest* 2011; **121**: 3804–9. doi: https://doi.org/10.1172/JCI57099
13. de Kruijf EM, van Nes JGH, van de Velde CJH, Putter H, Smit VTHBM, Liefers GJ, et al. Tumor-Stroma ratio in the primary tumor is a prognostic factor in early breast cancer patients, especially in triple-negative carcinoma patients. *Breast Cancer Res Treat* 2011; **125**: 687–96. doi: https://doi.org/10.1007/s10549-010-0855-6
14. Dekker TJA, van de Velde CJH, van Pelt GW, Kroep JR, Julien J-P, Smit VTHBM, et al. Prognostic significance of the tumor-stroma ratio: validation study in node-negative premenopausal breast cancer patients from the EORTC perioperative chemotherapy (POP) trial (10854. *Breast Cancer Res Treat* 2013; **139**: 371–9. doi: https://doi.org/10.1007/s10549-013-2571-5
15. Moorman AM, Vink R, Heijmans HJ, van der Palen J, Kouwenhoven EA. The prognostic value of tumour-stroma ratio in triple-negative breast cancer. *Eur J Surg Oncol* 2012; **38**: 307–13. doi: https://doi.org/10.1016/j.ejso.2012.01.002
16. Kramer CJH, Vangangelt KMH, van Pelt GW, Dekker TJA, Tollenaar RAEM, Mesker WE, et al. The prognostic value of tumour-stroma ratio in primary breast cancer with special attention to triple-negative tumours: a review. *Breast Cancer Res Treat* 2019; **173**: 55–64. doi: https://doi.org/10.1007/s10549-018-4987-4
17. Park VY, Kim E-K, Kim MJ, Yoon JH, Moon HJ. Perfusion parameters on breast dynamic contrast-enhanced MRI are associated with

disease-specific survival in patients with triple-negative breast cancer. *AJR Am J Roentgenol* 2017; **208**: 687–94. doi: https://doi.org/10.2214/AJR.16.16476
18. Nagasaka K, Satake H, Satoko Ishigaki ·, et al. Histogram analysis of quantitative pharmacokinetic parameters on DCE-MRI: correlations with prognostic factors and molecular subtypes in breast cancer. *Breast Cancer* 2018; **0**: 3.
19. Pickles MD, Lowry M, Manton DJ, Turnbull LW. Prognostic value of DCE-MRI in breast cancer patients undergoing neoadjuvant chemotherapy: a comparison with traditional survival indicators. *Eur Radiol* 2015; **25**: 1097–106. doi: https://doi.org/10.1007/s00330-014-3502-5
20. Blaschke E, Abe H. Mri phenotype of breast cancer: kinetic assessment for molecular subtypes. *J Magn Reson Imaging* 2015; **42**: 920–4. doi: https://doi.org/10.1002/jmri.24884
21. Li SP, Padhani AR, Taylor NJ, Beresford MJ, Ah-See M-LW, Stirling JJ, et al. Vascular characterisation of triple negative breast carcinomas using dynamic MRI. *Eur Radiol* 2011; **21**: 1364–73. doi: https://doi.org/10.1007/s00330-011-2061-2
22. Koo HR, Cho N, Song IC, Kim H, Chang JM, Yi A, et al. Correlation of perfusion parameters on dynamic contrast-enhanced MRI with prognostic factors and subtypes of breast cancers. *J Magn Reson Imaging* 2012; **36**: 145–51. doi: https://doi.org/10.1002/jmri.23635
23. Yamaguchi K, Hara Y, Kitano I, Hamamoto T, Kiyomatsu K, Yamasaki F, et al. Tumor-Stromal ratio (Tsr) of invasive breast cancer: correlation with multi-parametric breast MRI findings. *Br J Radiol* 2019; **92**: 20181032. doi: https://doi.org/10.1259/bjr.20181032
24. Chen W, Giger ML, Lan L, Bick U. Computerized interpretation of breast MRI: investigation of enhancement-variance dynamics. *Med Phys* 2004; **31**: 1076–82. doi: https://doi.org/10.1118/1.1695652
25. Wood C. Computer aided detection (CAD) for breast MRI. *Technol Cancer Res Treat* 2005; **4**: 49–53. doi: https://doi.org/10.1177/153303460500400107
26. Kim JJ, Kim JY, Kang HJ, Shin JK, Kang T, Lee SW, et al. Computer-Aided Diagnosis-generated kinetic features of breast cancer at preoperative MR imaging: association with disease-free survival of patients with primary operable invasive breast cancer. *Radiology* 2017; **284**: 45–54. doi: https://doi.org/10.1148/radiol.2017162079
27. Nam SY, Ko ES, Lim Y, Han B-K, Ko EY, Choi JS, et al. Preoperative dynamic breast magnetic resonance imaging kinetic features using computer-aided diagnosis: association with survival outcome and tumor aggressiveness in patients with invasive breast cancer. *PLoS One* 2018; **13**: e0195756. doi: https://doi.org/10.1371/journal.pone.0195756
28. Dietzel M, Zoubi R, Vag T, Gajda M, Runnebaum IB, Kaiser WA, et al. Association between survival in patients with primary invasive breast cancer and computer aided MRI. *J Magn Reson Imaging* 2013; **37**: 146–55. doi: https://doi.org/10.1002/jmri.23812
29. Jafri NF, Newitt DC, Kornak J, Esserman LJ, Joe BN, Hylton NM, et al. Optimized breast MRI functional tumor volume as a biomarker of recurrence-free survival following neoadjuvant chemotherapy. *J Magn Reson Imaging* 2014; **40**: 476–82. doi: https://doi.org/10.1002/jmri.24351
30. Hylton NM, Gatsonis CA, Rosen MA, Lehman CD, Newitt DC, Partridge SC, et al. Neoadjuvant chemotherapy for breast cancer: functional tumor volume by MR imaging predicts recurrence-free Survival-Results from the ACRIN 6657/CALGB 150007 I-SPY 1 trial. *Radiology* 2016; **279**: 44–55. doi: https://doi.org/10.1148/radiol.2015150013
31. Lo W-C, Li W, Jones EF, Newitt DC, Kornak J, Wilmes LJ, et al. Effect of imaging parameter thresholds on MRI prediction of neoadjuvant chemotherapy response in breast cancer subtypes. *PLoS One* 2016; **11**: e0142047. doi: https://doi.org/10.1371/journal.pone.0142047
32. Hammond MEH, Hayes DF, Dowsett M, Allred DC, Hagerty KL, Badve S, et al. American Society of clinical Oncology/College of American pathologists guideline recommendations for immunohistochemical testing of estrogen and progesterone receptors in breast cancer. *JCO* 2010; **28**: 2784–95. doi: https://doi.org/10.1200/JCO.2009.25.6529
33. Wolff AC, Hammond MEH, Schwartz JN, Hagerty KL, Allred DC, Cote RJ, et al. American Society of clinical Oncology/College of American pathologists guideline recommendations for human epidermal growth factor receptor 2 testing in breast cancer. *Arch Pathol Lab Med* 2007; **131**: 118–45. doi: https://doi.org/10.1200/JCO.2006.09.2775
34. Tuncbilek N, Tokatli F, Altaner S, Sezer A, Türe M, Omurlu IK, et al. Prognostic value DCE-MRI parameters in predicting factor disease free survival and overall survival for breast cancer patients. *Eur J Radiol* 2012; **81**: 863–7. doi: https://doi.org/10.1016/j.ejrad.2011.02.021
35. Toi M, Inada K, Suzuki H, Tominaga T. Tumor angiogenesis in breast cancer: its importance as a prognostic indicator and the association with vascular endothelial growth factor expression. *Breast Cancer Res Treat* 1995; **36**: 193–204. doi: https://doi.org/10.1007/BF00666040
36. Uzzan B, Nicolas P, Cucherat M, Perret G-Y. Microvessel density as a prognostic factor in women with breast cancer: a systematic review of the literature and meta-analysis. *Cancer Res* 2004; **64**: 2941–55. doi: https://doi.org/10.1158/0008-5472.can-03-1957
37. Gasparini G. Prognostic value of vascular endothelial growth factor in breast cancer. *Oncologist* 2000; **5 Suppl 1**(Suppl 1): 37–44. doi: https://doi.org/10.1634/theoncologist.5-suppl_1-37
38. Yim H, Kang DK, Jung YS, Jeon GS, Kim TH. Analysis of kinetic curve and model-based perfusion parameters on dynamic contrast enhanced MRI in breast cancer patients: correlations with dominant stroma type. *Magn Reson Imaging* 2016; **34**: 60–5. doi: https://doi.org/10.1016/j.mri.2015.07.010
39. Ku YJ, Kim HH, Cha JH, Shin HJ, Chae EY, Choi WJ, et al. Predicting the level of tumor-infiltrating lymphocytes in patients with triple-negative breast cancer: usefulness of breast MRI computer-aided detection and diagnosis. *J Magn Reson Imaging* 2018; **47**: 760–6. doi: https://doi.org/10.1002/jmri.25802
40. Adams S, Gray RJ, Demaria S, Goldstein L, Perez EA, Shulman LN, et al. Prognostic value of tumor-infiltrating lymphocytes in triple-negative breast cancers from two phase III randomized adjuvant breast cancer trials: ECoG 2197 and ECoG 1199. *JCO* 2014; **32**: 2959–66. doi: https://doi.org/10.1200/JCO.2013.55.0491
41. Ibrahim EM, Al-Foheidi ME, Al-Mansour MM, Kazkaz GA. The prognostic value of tumor-infiltrating lymphocytes in triple-negative breast cancer: a meta-analysis. *Breast Cancer Res Treat* 2014; **148**: 467–76. doi: https://doi.org/10.1007/s10549-014-3185-2
42. Uematsu T. Focal breast edema associated with malignancy on T2-weighted images of breast MRI: peritumoral edema, prepectoral edema, and subcutaneous edema. *Breast Cancer* 2015; **22**: 66–70. doi: https://doi.org/10.1007/s12282-014-0572-9
43. Uematsu T, Kasami M, Watanabe J. Is evaluation of the presence of prepectoral edema on T2-weighted with fat-suppression 3 T breast MRI a simple and readily available noninvasive technique for estimation of prognosis in patients with breast cancer?

Breast Cancer 2014; **21**: 684–92. doi: https://doi.org/10.1007/s12282-013-0440-z

44. Cheon H, Kim HJ, Lee SM, Cho SH, Shin KM, Kim GC, et al. Preoperative MRI features associated with lymphovascular invasion in node-negative invasive breast cancer: a propensity-matched analysis. *J Magn Reson Imaging* 2017; **46**: 1037–44. doi: https://doi.org/10.1002/jmri.25710
45. Bae MS, Shin SU, Ryu HS, Han W, Im S-A, Park I-A, et al. Pretreatment MR imaging features of triple-negative breast cancer: association with response to neoadjuvant chemotherapy and recurrence-free survival. *Radiology* 2016; **281**: 392–400. doi: https://doi.org/10.1148/radiol.2016152331
46. Jansen SA, Shimauchi A, Zak L, Fan X, Wood AM, Karczmar GS, et al. Kinetic curves of malignant lesions are not consistent across MRI systems: need for improved standardization of breast dynamic contrast-enhanced MRI acquisition. *AJR Am J Roentgenol* 2009; **193**: 832–9. doi: https://doi.org/10.2214/AJR.08.2025
47. Bolouri MS, Elias SG, Wisner DJ, Behr SC, Hawkins RA, Suzuki SA, et al. Triple-Negative and non-triple-negative invasive breast cancer: association between Mr and fluorine 18 fluorodeoxyglucose PET imaging. *Radiology* 2013; **269**: 354–61. doi: https://doi.org/10.1148/radiol.13130058